Published in final edited form as:
J Pathol. 2012 December ; 228(4): 448–458. doi:10.1002/path.4067.

Loss of Glutathione S-transferase A4 Accelerates Obstruction-induced Tubule Damage and Renal Fibrosis

Anlin Liang[1,2], **Yun Wang**[1], **Lauren E. Woodard**[1], **Matthew H. Wilson**[1,5], **Rajendra Sharma**[3], **Yogesh C. Awasthi**[3], **Jie Du**[4], **William E. Mitch**[1], and **Jizhong Cheng**[1,*]

[1]Nephrology Division, Baylor College of Medicine, Houston, Texas 77030, USA

[2]Department of Orthopedics, First Affiliated Hospital of Chongqing Medical University, 1st Youyi Road, Yuzhong District, Chongqing 400016, China

[3]Department of Molecular Biology and Immunology, University of North Texas Health Science Center, 3500 Camp Bowie Boulevard, Fort Worth, TX 76107, USA

[4]Beijing Anzhen Hospital, The Key Laboratory of Remodeling-related Cardiovascular Diseases, Capital Medical University, Ministry of Education, Beijing 100029, China

[5]Michael E. DeBakey VA Medical Center, Houston, TX 77030, USA

Abstract

Glutathione transferase isozyme A4 (GSTA4) exhibits high catalytic efficiency to metabolize 4-hydroxynonenal (4-HNE), a highly reactive lipid peroxidation product that has been implicated in the pathogenesis of various chronic diseases. Present studies were designed to elucidate the role of 4-HNE in the mechanisms of unilateral ureteral obstruction (UUO) induced fibrosis and its modulation by GSTA4–4 in a mouse model. Results of these studies indicated that after UUO, accumulation of 4-HNE and its adducts were increased in renal tissues with a concomitant decrease in the expression of GSTA4–4 in mice. As compared to the wild type (WT) mice, UUO caused an increased expression of fibroblast markers in the interstitium of *GSTA4* KO mice. Additionally, increased autophagy and tubular cell damage were more severe in the UUO-treated *GSTA4* KO mice as compared to the WT mice. Furthermore, the GSK-3β phosphorylation and expression of Snail, a regulator of E-cadherin and Occludin, was found to be significantly higher in the UUO-inflicted *GSTA4* KO mice. GSTA4 overexpression prevented 4-HNE-induced autophagy activation, tubular cell damage and Snail nuclear translocation *in vitro*. Effects of long-term expression of *GSTA4* in restoration of the UUO-induced damage in mice with the *GSTA4* inducible transposon system indicated that release of obstruction after 3 days of UUO resulted in the attenuation of the interstitial SMA-α and collagen I expression. This transposon-delivered GSTA4 expression also suppressed UUO-induced loss of tubular cell junction markers and autophagy activation. Together, these results for the first time indicated that 4-HNE significantly

Corresponding Author: Dr. Jizhong Cheng, jizhongc@bcm.edu.

Statement of author contribution:
AL, YW, LW, and JC carried out experiments, study design, and data analysis. JC, MW, and JD searched the literature and interpreted the data. JC, RS, WM, and LW were involved in writing the paper. All authors had final approval of the submitted and published versions.

contributes to the mechanisms of tubule injury and fibrosis and these effects can be inhibited by the enhanced expression of GSTA4–4.

Keywords

glutathione S-transferase; 4-hydroxynonenal; renal fibrosis; autophagy; junction molecule; obstructive nephropathy

Introduction

Obstructive nephropathy is a primary cause of renal disease in children, and in adults, its incidence increases in patients 60–65 years of age. Understanding the underlying mechanisms of the interstitial fibrosis and tubular atrophy that develop with obstruction could lead to methods to prevent loss of kidney function [1,2]. Unilateral ureteral obstruction (UUO) in mice or rats is associated with tubulointerstitial fibrosis, cellular infiltration, tubular proliferation, and apoptosis [3,4]. The fibrosis generated by UUO is linked to reactive oxygen species (ROS) generated at sites of inflammation and injury, initiating polyunsaturated lipid peroxidation (LPO) and contributing to the development of renal fibrosis [3,4]. The most abundant product and one of the most biologically active aldehydes generated during membrane LPO is 4-hydroxynonenal (4-HNE). During oxidative stress 4-HNE can accumulate, reaching 10 μM to 5 mM in certain tissues [5,6]. It acts primarily by forming adducts with proteins, producing functional alterations [7,8]. For example, 4-HNE can interact with cadherin and tight junction molecules producing endothelial barrier dysfunction [9] and in renal tubules it is associated with the induction of endoplasmic reticulum stress [10].

In cells, 4-HNE is predominantly metabolized by the Phase II detoxification enzymes glutathione S-transferases (GSTs) by its conjugation to glutathione (GSH) [11]. The catalytic efficiency of different GST isozymes is varied towards 4-HNE, while a subgroup of the α-class GSTs, GSTA4–4 isoform, has about two orders of magnitude higher activity towards 4-HNE than the other GST isoforms [12–14].

Several findings suggest that 4-HNE significantly contributes in the alteration of cellular functions. Previously, we have demonstrated that the overexpression of murine GSTA4 in K562 cells led to as much as a 90% decrease in the level of cellular 4-HNE [15]. Furthermore, the treatment of K562 and HL60 cells with 10–20 μM 4-HNE causes apoptosis which is blocked by GSTA4 overexpression [15,16]. In *Caenorhabditis elegans*, knockout (KO) *GSTA4* results in a shorter lifespan and mice with *GSTA4* KO exhibit age-dependent obesity [17,18]. These results suggest that GSTA4 can protect cells or animals from 4-HNE-induced oxidative stress.

During the present studies, we explored the influence of GSTA4 on UUO-induced fibrosis and modulated the levels of GSTA4 in kidneys using a transposon-based approach to integrate the *GSTA4* gene *in vivo* [19,20]. The therapeutic role of GSTA4 was examined by using a transposon-based inducible gene expression system in the mice. We also studied UUO in *GSTA4* KO mice and found accelerated fibrosis plus autophagy activation and

tubular cell damage, which were regulated through 4-HNE-stimulated activation of the GSK3β/Snail signaling pathway. Our results indicate that increasing the expression and functions of GSTA4 can suppress the UUO-induced fibrosis in the mouse kidney through inhibition of oxidative stress.

Materials and Methods

Plasmids and adenoviruses preparation

The adenovirus *mGSTA4* expression vector was constructed by inserting the *mGSTA4* cDNA into pTracker-CMV vector and the adenovirus was prepared as before [21]. The pT-TetOn, pT-tight-Luc, and pCMV-*piggyBac* transposon plasmids have been described previously [20] and pcDNA3-*mGSTA4* was constructed as described [16]. pT-tight-*mGSTA4* was made by digesting pcDNA3-mGSTA4 with *Eco*RI to release the *mGSTA4* reading frame and pT-tight-Luc with *Xma*I and *Nhe*I to remove the luciferase gene. The digested plasmids were treated with Klenow Large Fragment (New England Biolabs, Ipswich, MA) to create blunt ends and the pT-tight backbone fragment was dephosphorylated using Antarctic Phosphatase (New England Biolabs). After gel purification, the fragments were ligated via Quick Ligase (New England Biolabs) and the final construct was confirmed by sequencing. All plasmids were prepared to be endotoxin free (Qiagen, Valencia, CA).

Animals

Male WT and *GSTA4* KO mice [22] weighing 20 to 22 g were subjected to UUO as described and compared to sham-operated mice [21]. At different times groups of mice (n = 5) were anaesthetized and the kidneys were removed for various analyses. Animal protocols (AN-4599 and D1557) were approved by the Institutional Animal Care and Use Committee at the Baylor College of Medicine.

Release of UUO

GSTA4 KO and WT male mice (6- to 8-wk-old) were used. Under anesthesia, the right ureter was isolated and clamped with a nontraumatic microvascular clip (5–15 g/mm^2, 7 mm S&T Vascular Clamp; Fine Science Tools, Foster City, CA) for 3 days. UUO was released by removing the microvascular clamp. The success of the release of the obstruction was confirmed by observation of the renal pelvis. To induce *GSTA4* expression, the plasmids pCMV-*piggyBac*, pT-TetOn, and pT-tight-GSTA4 were mixed with endotoxin-free hydrodynamic injection solution QR (Mirus, Madison, WI) and injected into the renal vein of one kidney. Subsequently, UUO was created and released 3 days later. Doxycyclin (2 mg/ml) was added to drinking water when the ureteral obstruction was released. Three weeks later, animals were sacrificed and the kidneys were analyzed.

4-Hydroxynonenal quantification

4-HNE in mouse kidneys was determined using the OxisSelect HNE-His Adduct ELISA Kit (Cat# STA 338, Cell Biolab, San Diego, CA) according to the manufacturer's protocol. By using this kit instead of free 4-HNE, the conjugated HNE-His proteins were detected. A series of 4-HNE-BSA standards was prepared for each determination. Wild-type and

GSTA4 KO mouse kidneys were rinsed twice with cold PBS and homogenized to a 20% (w/v) mixture. The homogenates were centrifuged at 13000 × g for 15 min and 0.2 ml of the supernatants was used for each determination according to the manufacturer's instructions. Each sample was diluted to 10 μg/ml in 1 × PBS. After binding to the 96-well plate at 4°C overnight, the samples were incubated with anti-HNE-His antibody and then incubated for 1 hour at room temperature. Then, the reaction mixtures were incubated with secondary antibody-HRP conjugate at room temperature for 1 hour. After the enzyme reaction was stopped by the addition of stop solution, the absorbance of the supernatants was determined at 450 nm.

Antibodies

Antibodies against pGSK3β were purchased from Cell Signaling Technology (Beverly, MA), against Collagen I from Abcam (Cambridge, MA) and against TGF-β1, Snail, Beclin 1, and GAPDH from Santa Cruz Biotechnology (Santa Cruz, CA). The anti-SMA-α antibody was purchased from Sigma, Inc (Sigma-Aldrich, Louis, MO), the FSP-1 antibody from DAKO (Carpenteria, CA), and the LC3-II antibody from Novus Biologicals (Littleton, CO). The anti-mouse GSTA4 antibody was generated from rabbit [16].

Immunohistochemistry

For histological analysis, the kidneys were prepared by perfusion of the mice through the left ventricle and slides of the kidney were prepared as described [21]. The slides were fixed for 24 h using 4% phosphate-buffered formaldehyde at 4°C and subsequently processed as described [23]. Sections were blocked with 10% goat serum (Vector Laboratories, Burlingame, CA) for 30 min and then incubated with the primary antibodies. Sections were washed in 0.5% Tween 20 in PBS (PBST) and incubated with a biotinylated secondary antibody (Vector Laboratories) at room temperature. After PBST washes, tissue sections were incubated with an *Elite®* ABC reagent (Vector Laboratories) followed by a peroxidase substrate kit (Vector Laboratories) according to the manufacturer's protocol. The sections were counterstained by hematoxylin. For double immunofluorescence staining, fluorescent secondary antibodies were applied to sections and 4′,6-diamidino-2-phenylindole (DAPI) was used to stain the nuclear DNA. The Nikon Eclipse 80i fluorescence microscope (Melville, NY) was used to capture the images and the negative control was either an isotype-matched IgG or PBST. The areas of positive signal were measured using the NIS-Elements BR 3.0 program.

Real-time RT-PCR

Total kidney RNA was isolated by the RNeasy kit (Qiagen, Valencia, CA). Real-time RT-PCR was performed with the Opticon real-time RT-PCR machine (MJ Research, Waltham, MA). The RT-PCR results were confirmed by agarose gel electrophoresis and melting-curve analysis. *GAPDH* was used as an internal standard. The primers used were mouse *FSP-1* (forward 5′-TTCCAGAAGGTGATGAG-3′ and reverse 5′-TCATGGCAATGCAGGACAGGAAGA-3′), *GSTA4* (forward primer: 5′-CGGCCA AGTACCCTTGGTTGAAAT-3′ and reverse 5′-AATGGAGCCACGGCAATCATCATC-3′), *SMA-α* (forward 5′-CTGACAGAGGCACCACTGAA-3′ and reverse 5′-GAAATAGCC AAGCTCAG-3′) and

GAPDH (forward 5′-AGTGGGAGTTGCTGTTGAAATC-3′ and reverse 5′-TGCTGAGTATGTCGTGGA GTCTA-3′).

Cell culture

Mouse tubular cells from WT and *GSTA4* KO mice were isolated as previously described[21] and cultured in DMEM supplemented with 10% heat-inactivated fetal bovine serum (Hyclone, Logan, UT), 100 μg/mL penicillin, and 100 μg/mL streptomycin (Invitrogen Life Technologies, Carlsbad, CA). The cells were serum starved for 24 h before 4-HNE (10–25 μM) was added, then cells were fixed for immunofluorescencestaining or lysed in RIPA buffer for Western blot analysis.

Western blot analysis

The cell extracts were prepared in RIPA buffer, protein concentration in the extracts was determined by Bradford protein assay kit (BioRad, Hercules, CA), and ~30 μg of protein was separated by SDS-PAGE. After transferring to nitrocellulose membranes, immunoblots were probed separately with various primary antibodies after blocking with 5% skim milk in TBS. Fluorescently labeled secondary antibodies were used for detection by the Odyssey Infrared Imaging System (LI-COR, Inc, Lincoln, Nebraska, USA).

Transmission electron microscopy

Mice were sacrificed at 7 days after UUO or sham operation. The kidneys were perfused with PBS and fixed by immersion in 0.1 M cacodylate buffer containing 2.5% glutaraldehyde. Samples were dehydrated through ascending grades of ethanol, embedded, sectioned (90 nm thick), and stained with lead citrate and 2% aqueous uranyl acetate. They were dehydrated through ascending grades of ethanol. Samples were examined with the JEM-1200 transmission electron microscope in the Baylor College of Medicine core facility.

Statistical analysis

All data are presented as the mean ± standard error of the mean (SEM). Comparison between groups was made using one-way ANOVA; $P < 0.05$ was considered to be statistically significant.

Results

UUO suppresses GSTA4 expression and increases 4-HNE

A high level of GSTA4 was observed in western blots of normal kidneys (Fig. 1A). After UUO, the mRNA and protein levels of GSTA4 were decreased (~70%) compared to values in the contralateral kidney (Fig. 1B & C). There was also a significant increase in 4-HNE-protein conjugates in lysates of whole kidneys following UUO (Fig. 1D). These changes were associated with increased 4-HNE protein adducts in obstructed *vs* control kidneys (Fig. 1E). After UUO, immunostaining indicated that tubular cells stained positive for 4-HNE-protein conjugates; however, compared to the WT mice with UUO, there was an increased accumulation of 4-HNE-protein conjugates in the obstructed kidney of *GSTA4* KO mice (Fig. 1F).

UUO induces interstitial fibroblast markers in kidneys of GSTA4 KO mice

The expression of SMA-α and fibroblast specific protein 1 (FSP-1) is induced when fibroblasts become myofibroblasts, and both molecules have been used as markers for fibrosis [24, 25]. After UUO, the number of SMA-α positive cells increased in a time-dependent manner which were further enhanced in kidneys of *GSTA4* KO mice (Fig. 2A). Similar results were obtained when FSP-1 levels were examined (Fig. 2B). These responses were confirmed in measurements of protein levels of FSP-1 and SMA-α (Fig. 2C). UUO increased the levels of mRNA for these fibroblast markers in the kidneys of *GSTA4* KO mice when compared with those of WT mice (Fig. 2D & E).

GSTA4 KO enhances UUO-induced interstitial fibrosis in mice

Following UUO, PAS staining revealed that increased intensity of basement membrane staining was found in kidneys from *GSTA4* KO mice vs WT mice (Fig. 3A, red arrow). There also were morphology changes in the tubular cells with intracellular vacuolization in kidneys of *GSTA4* KO mice (Fig. 3A, green arrow). The internal vacuolization was found to be significantly high (>40 tubule cells/area) in *GSTA4* KO mice as compared to only a few observed in WT mice (Fig. 3B). In the interstitium, fibronectin was significantly increased in response to UUO in *GSTA4* KO mice (Fig. 3C). UUO markedly stimulated the expression of collagen I in a time dependent manner in both types of mice but collagen I expression was high in the kidneys of *GSTA4* KO mice as compared to WT mice (Fig. 3D & E).

GSTA4 protects against 4-HNE-induced autophagy activation

After 7 days of UUO, tubular cells underwent autophagy as signified by double membrane vacuoles containing electron-dense material. In the contralateral kidney, there was no autophagy or abnormalities in tubular cells (Fig. 4A). An increased conversion of microtubule-associated protein 1 light-chain 3 (LC3) has been observed during autophagy and the expression of LC3-II represents biochemical evidence of autophagy in mammalian cells, consistent with this, we found higher expression of UUO-induced LC3-II in kidneys from *GSTA4* KO mice than in WT mice (Fig. 4B). UUO has also been shown to increase the expression of another autophagy marker Beclin 1 [26, 27]. Results presented in Fig. 4B showed higher expression of Beclin 1 in GSTA4 KO when compared with WT mice after the induction of UUO. While 4-HNE treatment further stimulated LC3-II expression in tubular cells isolated from *GSTA4* KO mice, overexpression of GSTA4 in these cells blocked 4-HNE-induced autophagy activation (Fig. 4C).

GSTA4 protects against 4-HNE-induced tubular cell junction molecule loss in vitro

ECM analysis showed that increased junction structure loss between tubular cells was present in UUO kidneys of *GSTA4* KO mice (Fig. 5A). We examined TEM images and found that UUO was associated with loss of tubular cell microvilli, a decrease in mitochondria close to nuclei and a decrease in the junction structures. These changes were more prominent in tubule cells of *GSTA4* KO mice (Fig. 5B). In cultured mouse tubular cells, 4-HNE attenuated E-cadherin and Occludin expression, which was inhibited by the ectopic overexpression of GSTA4 in these cells (Fig. 5C). One of the mechanisms for these

responses is mediated by the transcription factor Snail and its upstream kinase GSK3β which can negatively regulate Occludin and E-cadherin [28]. We found that 4-HNE increased the phosphorylation of GSK3β in a dose-dependently manner (Fig. 5D). Exposure to 4-HNE induced the expression of Snail and pGSK3β in *GSTA4* KO cells when compared with their expression levels in WT cells; ectopic rescue of GSTA4 expression in *GSTA4* KO cells prevented these effects of 4-HNE (Fig. 5E). Overexpression of GSTA4 also blocked 4-HNE-mediated snail nuclear accumulation (Fig. 5F).

Transposon-mediated inducible GSTA4 expression suppresses UUO-induced fibrosis

To explore the potential for a therapeutic role of GSTA4 toward obstructive renal injury, we transferred an inducible *GSTA4* gene into the kidney and later subjected it to UUO to induce interstitial fibrosis. We then released the ureteral obstruction and added doxycycline to induce GSTA4. The gene transfer was accomplished using a transposon system to integrate the *GSTA4* gene into the genomic DNA so as to achieve long-term gene expression. The inducible tet-on system was employed to delay expression of GSTA4 until after UUO release (Fig. 6A). Initially, we confirmed that this system mediates inducible expression of GSTA4 in cultured HEK293 kidney cells where GSTA4 expression was induced in a dose-dependent manner by doxycycline treatment (Fig. 6B). The experimental plan is shown in Fig. 6C. To examine how GSTA4 might influence renal fibrosis, the transposon plasmids were injected into the renal vein and 2 weeks later, the ureter was obstructed for 3 days and then released. At day 3 after releasing UUO, tubules were still inflated but this change was corrected by 2 weeks (Fig. 6D). SMA-α continued to rise even after release of the obstruction and at 3 weeks after release of UUO, the SMA-α level decreased (Fig. 6E). After 3 weeks, assessment of *GSTA4* mRNA expression by real time RT-PCR indicated that *GSTA4* mRNA increased 7-fold following induction by doxycycline *in vivo* vs *GSTA4* levels in vector-treated control kidneys (Fig. 6F).

GSTA4 expression accelerates recovery of UUO-induced fibrosis

At 3 weeks after doxycycline was used to induce GSTA4 expression, the level of 4-HNE in the kidneys was lower as compared to those treated with control plasmids (Fig. 7A). Notably, there was a significant reduction of SMA-α and Collagen I expression in GSTA4 overexpression mice compared with vector treated mice following release of UUO (Fig. 7B–D).

GSTA4 expression protects against UUO-induced tubular cell damages

Since the UUO and 4-HNE induced autophagy and junction molecule loss in tubular cells, we therefore analyzed whether overexpression of GSTA4 can reverse these processes *in vivo*. Overexpression of GSTA4 in kidneys subjected to UUO had reduced LC3-II expression (Fig. 8A). We found that overexpression of GSTA4 prevented UUO-mediated decreases in the levels of Occludin and E-cadherin (Fig. 8B & C). The UUO increased GSK-3β phosphorylation and Snail expression in tubular cells; overexpression of GSTA4 blocked UUO-induced changes in pGSK-3β and Snail (Fig. 8D & E). Increased GSK-3β phosphorylation induces Snail accumulation. We found that UUO increases Snail expression and nuclear localization in tubular cells (Fig. 8F). These changes were accelerated in *GSTA4* KO mice but were ameliorated in GSTA4 overexpressing mice (Fig. 8F).

Discussion

A major mechanism for tubular cell dysfunction and the development of fibrosis is oxidative damage. For example, UUO was shown to induce tubular cell atrophy and when tubular cell apoptosis was inhibited, there was protection against kidney damage and the development of fibrosis [29]. The highly reactive aldehyde 4-HNE, is generated during oxidative degradation of fatty acids including arachidonic and linoleic acids [5]. Increased levels of 4-HNE in the kidney have been found following lipid peroxidation [30]. We found that following UUO, 4-HNE is increased in the kidney and reaches even higher levels in mice lacking *GSTA4*. This is relevant because UUO induced-tubule morphologic changes and fibrosis can be suppressed by the overexpression of GSTA4. Our results suggest that 4-HNE plays an important role in tubular cell damage and the initiation of fibrosis (Fig. 3A). Our results also suggest an effective strategy for counterbalancing high intracellular 4-HNE levels and the effects of UUO by utilizing a transposon-based gene delivery system to raise GSTA4 expression.

Autophagy is increasingly recognized as a factor influencing cellular homeostasis and in the kidney. Autophagy is increased during ischemia/reperfusion injury, transplant ischemia, and cis-platinum or cyclosporine toxicity [31]. We found that either by direct modulation of 4-HNE levels *in vitro* or through the induction of UUO *in vivo,* both activate autophagy in tubular cells, leading to a loss of cell function and the development of fibrosis. Since GSTA4 overexpression can decrease autophagy (Fig. 4C), our results are consistent with reports of Li, *et al* and others who have reported that UUO induces autophagy of tubule cells [31–33] and that 4-HNE stimulates autophagy in vascular smooth muscle cells [31,34].

We also found that high levels of 4-HNE induced by UUO significantly decrease the expression levels of E-cadherin and Occludin (Fig. 5). A potential mechanism for the changed expression of these epithelial markers involves Snail, a transcriptional repressor that suppresses E-cadherin and Occludin. Our earlier studies demonstrated that GSK-3β directly phosphorylates Snail [21]. *GSTA4* KO cells have a higher basal level of phosphorylated GSK-3β, especially following UUO (Fig. 4E). We propose that 4-HNE may initiate the phosphorylation of GSK3β, leading to accumulation of the transcriptional repressor, Snail. This in turn decreases levels of the junction molecules E-cadherin and Occuldin *in vivo* and *in vitro*. Overexpression of GSTA4 attenuates 4-HNE- and UUO-induced autophagy and tubular cell damage (Fig.5C & 8B). Since GSK-3 β can promote cell survival by modulating autophagy [35], our results suggest the both autophagy activation and modulation of the pGSK3β/Snail/E-cadherin pathway are involved in UUO-induced tubular cell atrophy.

Our results show that UUO produced a decrease in kidney GSTA4 content by approximately 70% (Fig. 1) that was accompanied by both enhanced intracellular vacuolization and the loss of junction molecules compared to WT mice subjected to UUO (Fig. 3B). The severity of tubular cell damage after UUO was followed by accelerated fibrosis in *GSTA4* KO mice (Fig. 3). Our preliminary unpublished data indicated that after 3 days of UUO, there is infiltration of macrophages, neutrophils, and monocytes into the interstitium. This would produce inflammation. At this time, GSTA4 expression was reduced (Figure 1B). These

results do not identify whether inflammation precedes or follows changes in GSTA4 nor do we know whether inflammation acts to stimulate GSTA4 or vice versa. There is evidence that inflammation could be an upstream event regulating GSTA4 expression. Since expression of GST can be regulated by pro-inflammatory agents and xenobiotics [36]. Alternatively, GSTA4 could act upstream to regulate inflammatory responses. For example, overexpression of GSTA4 decreased inflammation when 4-HNE production was blocked in a thermal injury in humans or mouse [37]. Possibly, GSTA4 plays a role in suppressing inflammation by limiting the 4-HNE production. Taken together, our results and others show that GSTA4 can protect against 4-HNE-induced decrease in junction molecules [38]. These findings highlight the importance of GSTA4 in maintaining tubular cell integrity and suggest that increasing the levels of GSTA4 protein could be beneficial in preventing the consequences of obstructive uropathy.

By using a transposon-based gene expression system to introduce the *GSTA4* expression plasmid DNA into mouse kidneys we were able to demonstrate stable overexpression of GSTA4 in kidney cells (Fig. 5). Non-integrating plasmid-based eukaryotic expression vectors create only transient expression lasting 5–7 days and therefore cannot effectively modulate the disease process long-term. With the present technique, we achieved a more stable transfection duo to genomic integration of the delivered transposon DNA [20, 39–41]. This was possible because we have previously shown that a single injection of transposons can produce long-term, inducible, gene expression *in vivo* (up to 120 days) [20]. In the present experiments, the levels of *mGSTA4* mRNA were 7-fold higher with transposon-mediated inducible expression (doxycycline) in the RUUO mouse model, compared to vector controls (Fig. 6). Importantly, the doxycycline-mediated induction of GSTA4 expression attenuated the development of fibrosis in this RUUO model.

In summary, we found that the reactive aldehyde, 4-HNE, plays a significant role in UUO-induced tubular cell damage and the development of kidney fibrosis. Accumulation of 4-HNE stimulated by UUO can increase autophagy and result in the loss of junction molecules through activation of the GSK-3β/Snail signaling pathway [21]. UUO-induced pathology was accelerated in *GSTA4* KO mice but was attenuated by the inducible expression of GSTA4. Our results indicate that anti-oxidative molecules/agents either applied directly or via transposon-based methods should be helpful in preventing the undesirable consequences of obstructive uropathy.

Acknowledgments

Sources of Funding

This study was supported by grants from the American Heart Association (10SDG2780009 to J.C.), grants from National Science Foundation of China (31090363, 30888004 to J.D.), the Veterans Administration (CDA-2 to M.H.W.), and a generous grant from Dr. and Mrs. Harold Selman. L.E.W. was supported by training grants from the National Institutes of Health (5T32DK062706 and 5T32DK604458).

Abbreviations

4-HNE 4-hydroxynonenal

GST	glutathione S-transferase
UUO	unilateral ureteral obstruction

References

1. Bascands JL, Schanstra JP. Obstructive nephropathy: insights from genetically engineered animals. Kidney Int. 2005; 68:925–937. [PubMed: 16105023]
2. Chevalier RL. Obstructive nephropathy: towards biomarker discovery and gene therapy. Nat Clin Pract Nephrol. 2006; 2:157–168. [PubMed: 16932414]
3. Zecher M, Guichard C, Velasquez MJ, et al. Implications of oxidative stress in the pathophysiology of obstructive uropathy. Urological research. 2009; 37:19–26. [PubMed: 19082822]
4. Gutteridge JM, Halliwell B. The measurement and mechanism of lipid peroxidation in biological systems. Trends in biochemical sciences. 1990; 15:129–135. [PubMed: 2187293]
5. Esterbauer H, Schaur RJ, Zollner H. Chemistry and biochemistry of 4-hydroxynonenal, malonaldehyde and related aldehydes. Free radical biology & medicine. 1991; 11:81–128. [PubMed: 1937131]
6. Uchida K. 4-Hydroxy-2-nonenal: a product and mediator of oxidative stress. Progress in lipid research. 2003; 42:318–343. [PubMed: 12689622]
7. Petersen DR, Doorn JA. Reactions of 4-hydroxynonenal with proteins and cellular targets. Free radical biology & medicine. 2004; 37:937–945. [PubMed: 15336309]
8. Dwivedi S, Sharma A, Patrick B, et al. Role of 4-hydroxynonenal and its metabolites in signaling. Redox Rep. 2007; 12:4–10. [PubMed: 17263900]
9. Usatyuk PV, Parinandi NL, Natarajan V. Redox Regulation of 4-Hydroxy-2-nonenal-mediated Endothelial Barrier Dysfunction by Focal Adhesion, Adherens, and Tight Junction Proteins. 2006:35554–35566.
10. Yeh CH, Chiang HS, Lai TY, et al. Unilateral ureteral obstruction evokes renal tubular apoptosis via the enhanced oxidative stress and endoplasmic reticulum stress in the rat. Neurourology and urodynamics. 2011; 30:472–479. [PubMed: 21305585]
11. Hayes JD, Pulford DJ. The glutathione S-transferase supergene family: regulation of GST and the contribution of the isoenzymes to cancer chemoprotection and drug resistance. Critical reviews in biochemistry and molecular biology. 1995; 30:445–600. [PubMed: 8770536]
12. Zimniak P, Singhal SS, Srivastava SK, et al. Estimation of genomic complexity, heterologous expression, and enzymatic characterization of mouse glutathione S-transferase mGSTA4–4 (GST 5. 7). J Biol Chem. 1994; 269:992–1000. [PubMed: 7904605]
13. Hubatsch I, Ridderstrom M, Mannervik B. Human glutathione transferase A4–4: an alpha class enzyme with high catalytic efficiency in the conjugation of 4-hydroxynonenal and other genotoxic products of lipid peroxidation. Biochem J. 1998; 330 (Pt 1):175–179. [PubMed: 9461507]
14. Cheng JZ, Yang Y, Singh SP, et al. Two distinct 4-hydroxynonenal metabolizing glutathione S-transferase isozymes are differentially expressed in human tissues. Biochem Biophys Res Commun. 2001; 282:1268–1274. [PubMed: 11302754]
15. Cheng JZ, Singhal SS, Saini M, et al. Effects of mGST A4 transfection on 4-hydroxynonenal-mediated apoptosis and differentiation of K562 human erythroleukemia cells. Arch Biochem Biophys. 1999; 372:29–36. [PubMed: 10562413]
16. Cheng JZ, Singhal SS, Sharma A, et al. Transfection of mGSTA4 in HL-60 cells protects against 4-hydroxynonenal-induced apoptosis by inhibiting JNK-mediated signaling. Arch Biochem Biophys. 2001; 392:197–207. [PubMed: 11488593]
17. Curtis JM, Grimsrud PA, Wright WS, et al. Downregulation of adipose glutathione S-transferase A4 leads to increased protein carbonylation, oxidative stress, and mitochondrial dysfunction. Diabetes. 59:1132–1142. [PubMed: 20150287]

18. Singh SP, Niemczyk M, Saini D, et al. Role of the electrophilic lipid peroxidation product 4-hydroxynonenal in the development and maintenance of obesity in mice. Biochemistry. 2008; 47:3900–3911. [PubMed: 18311940]
19. Cary LC, Goebel M, Corsaro BG, et al. Transposon mutagenesis of baculoviruses: analysis of Trichoplusia ni transposon IFP2 insertions within the FP-locus of nuclear polyhedrosis viruses. Virology. 1989; 172:156–169. [PubMed: 2549707]
20. Saridey SK, Liu L, Doherty JE, et al. PiggyBac transposon-based inducible gene expression in vivo after somatic cell gene transfer. Mol Ther. 2009; 17:2115–2120. [PubMed: 19809403]
21. Cheng J, Truong LD, Wu X, et al. Serum- and glucocorticoid-regulated kinase 1 is upregulated following unilateral ureteral obstruction causing epithelial-mesenchymal transition. Kidney Int. 2010; 78:668–678. [PubMed: 20631674]
22. Engle MR, Singh SP, Czernik PJ, et al. Physiological role of mGSTA4–4, a glutathione S-transferase metabolizing 4-hydroxynonenal: generation and analysis of mGsta4 null mouse. Toxicology and applied pharmacology. 2004; 194:296–308. [PubMed: 14761685]
23. Cheng J, Du J. Mechanical stretch simulates proliferation of venous smooth muscle cells through activation of the insulin-like growth factor-1 receptor. Arterioscler Thromb Vasc Biol. 2007; 27:1744–1751. [PubMed: 17541019]
24. Rossini M, Cheunsuchon B, Donnert E, et al. Immunolocalization of fibroblast growth factor-1 (FGF-1), its receptor (FGFR-1), and fibroblast-specific protein-1 (FSP-1) in inflammatory renal disease. Kidney Int. 2005; 68:2621–2628. [PubMed: 16316338]
25. Lan HY, Mu W, Tomita N, et al. Inhibition of Renal Fibrosis by Gene Transfer of Inducible Smad7 Using Ultrasound-Microbubble System in Rat UUO Model. J Am Soc Nephro. 2003; 14:1535–1548.
26. Cho DH, Jo YK, Hwang JJ, et al. Caspase-mediated cleavage of ATG6/Beclin-1 links apoptosis to autophagy in HeLa cells. Cancer Lett. 2009; 274:95–100. [PubMed: 18842334]
27. Takahashi Y, Coppola D, Matsushita N, et al. Bif-1 interacts with Beclin 1 through UVRAG and regulates autophagy and tumorigenesis. Nat Cell Biol. 2007; 9:1142–1151. [PubMed: 17891140]
28. Zhou BP, Deng J, Xia W, et al. Dual regulation of Snail by GSK-3[beta]-mediated phosphorylation in control of epithelial-mesenchymal transition. Nat Cell Biol. 2004; 6:931–940. [PubMed: 15448698]
29. Docherty NG, O'Sullivan OE, Healy DA, et al. Evidence that inhibition of tubular cell apoptosis protects against renal damage and development of fibrosis following ureteric obstruction. Am J Physiol Renal Physiol. 2006; 290:F4–13. [PubMed: 16339963]
30. Raguenez-Viotte G, Dieber-Rotheneder M, Dadoun C, et al. Evidence for 4-hydroxyalkenals in rat renal cortex peroxidized by N2-methyl-9-hydroxyellipticinium acetate or Celiptium. Biochim Biophys Acta. 1990; 1046:294–300. [PubMed: 2145981]
31. Li L, Zepeda-Orozco D, Black R, et al. Autophagy is a component of epithelial cell fate in obstructive uropathy. Am J Pathol. 176:1767–1778. [PubMed: 20150430]
32. Kim WY, Nam SA, Song HC, et al. The role of autophagy in unilateral ureteral obstruction rat model. Nephrology (Carlton, Vic). 2012; 17:148–159.
33. Forbes MS, Thornhill BA, Chevalier RL. Proximal tubular injury and rapid formation of atubular glomeruli in mice with unilateral ureteral obstruction: a new look at an old model. Am J Physiol Renal Physiol. 2011; 301:F110–117. [PubMed: 21429968]
34. Hill BG, Haberzettl P, Ahmed Y, et al. Unsaturated lipid peroxidation-derived aldehydes activate autophagy in vascular smooth-muscle cells. Biochem J. 2008; 410:525–534. [PubMed: 18052926]
35. Yang J, Takahashi Y, Cheng E, et al. GSK-3{beta} promotes cell survival by modulating Bif-1-dependent autophagy and cell death. J Cell Sci. 2010; 123:861–870. [PubMed: 20159967]
36. Higgins LG, Hayes JD. Mechanisms of induction of cytosolic and microsomal glutathione transferase (GST) genes by xenobiotics and pro-inflammatory agents. Drug metabolism reviews. 2011; 43:92–137. [PubMed: 21495793]
37. Apidianakis Y, Que Y-A, Xu W, et al. Down-regulation of glutatione S-transferase A4 (hGSTA4) in the muscle of thermally injured patients is indicative of susceptibility to bacterial infection. FASEB J. 2011; 26:730–737. [PubMed: 22038048]

38. Xu Y, Gong B, Yang Y, et al. Glutathione-S-transferase protects against oxidative injury of endothelial cell tight junctions. Endothelium. 2007; 14:333–343. [PubMed: 18080870]

39. Yant SR, Meuse L, Chiu W, et al. Somatic integration and long-term transgene expression in normal and haemophilic mice using a DNA transposon system. Nature genetics. 2000; 25:35–41. [PubMed: 10802653]

40. Nakanishi H, Higuchi Y, Kawakami S, et al. piggyBac Transposon-mediated Long-term Gene Expression in Mice. Mol Ther. 2010; 18:707–714. [PubMed: 20104210]

41. Hackett PB. Integrating DNA vectors for gene therapy. Mol Ther. 2007; 15:10–12. [PubMed: 17164769]

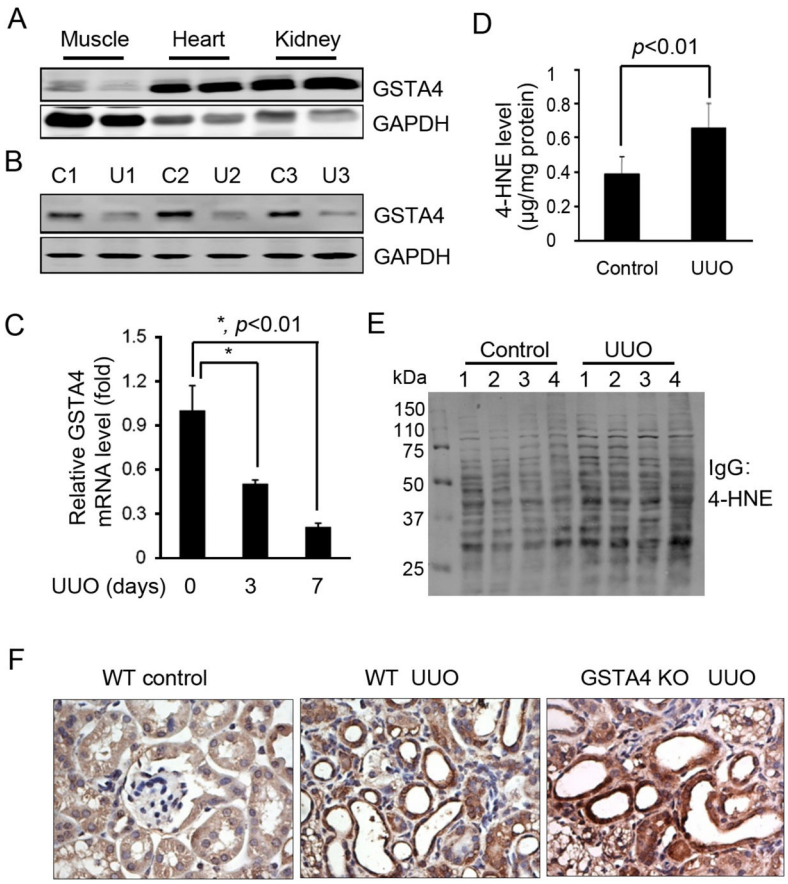

Figure 1.

UUO decreases GSTA4 expression and increases 4-HNE levels. A. GSTA4 expresses in the mouse kidney. Different tissues from mice were homogenized and Western blot was performed. B & C. Expression of GSTA4 protein and transcription are decreased in UUO. D. ELISA analysis of the concentration of 4-HNE in mouse kidneys after UUO for 3 days. Control lateral and UUO-treated kidneys were homogenized and the 4-HNE concentrations were analyzed by ELISA. E. UUO increases the formation of 4-HNE-protein adducts. F. The 4-HNE-adducts increased in UUO. 4-HNE levels in 7 day UUO mice were analyzed by immunostaining of WT and *GSTA4* KO kidney sections.

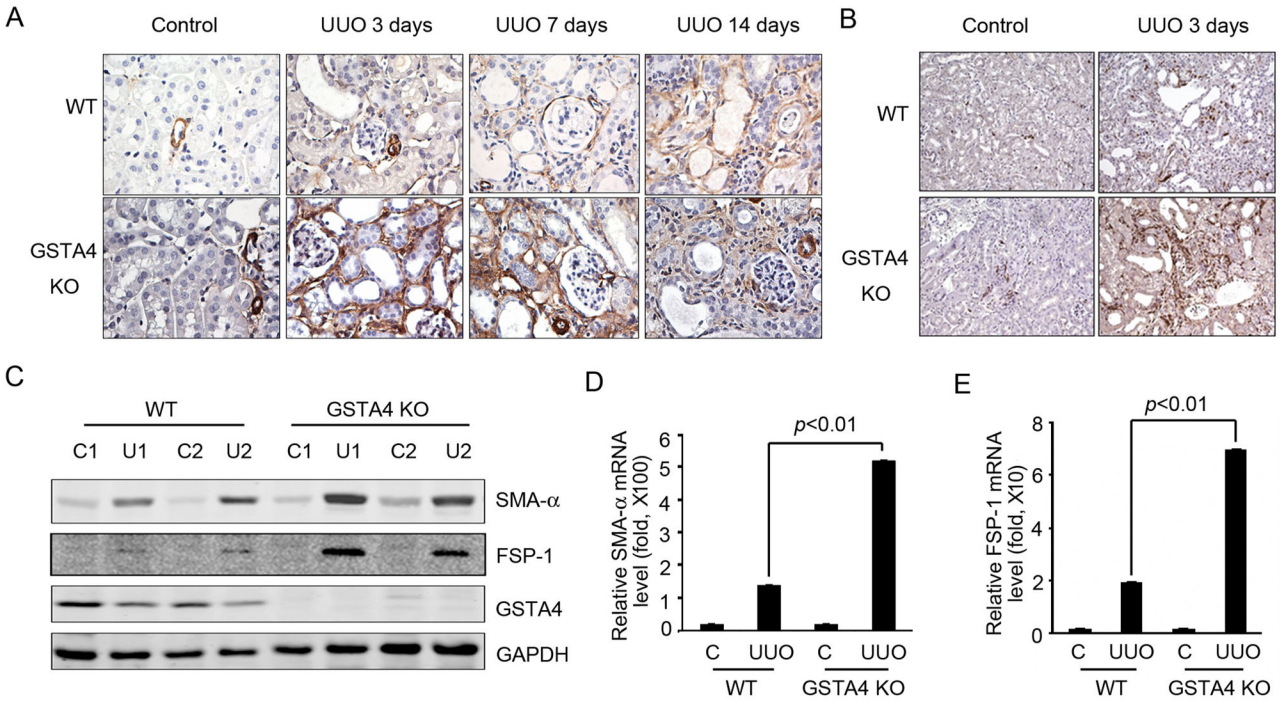

Figure 2.

GSTA4 KO increases UUO-induced expression of fibroblast markers in the interstitial area after UUO. A & B. expression of SMA-α (A) and FSP-1 (B) were analyzed by immunostaining of WT and *GSTA4* KO kidney sections. C-E, Western blots (C, D) and RT-PCR analysis (D, E) of SMA-α and FSP-1 expression in contralateral and 3 day UUO samples in WT and *GSTA4* KO mice. The data shown were representative of 3 repeated experiments.

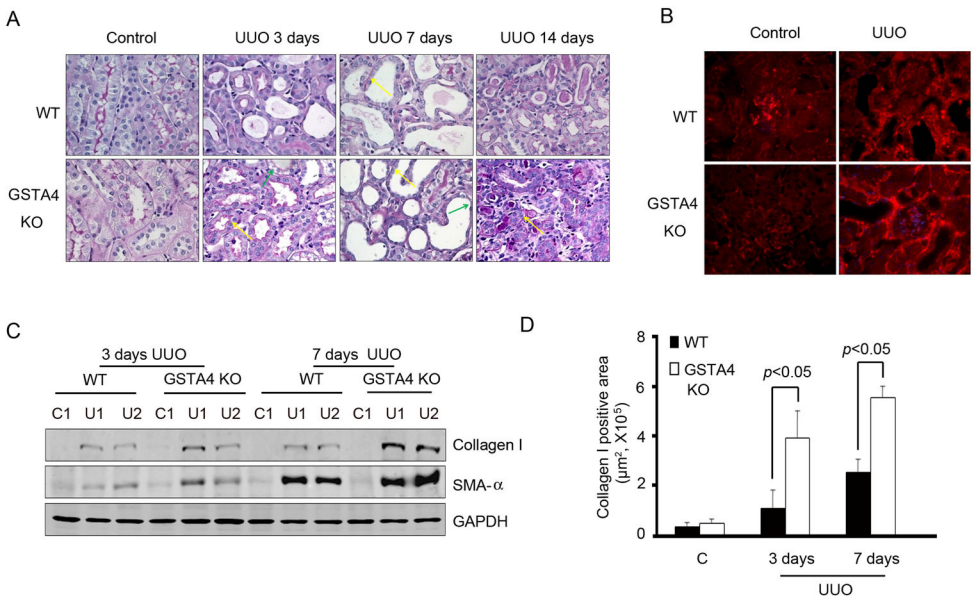

Figure 3.

GSTA4 KO enhances UUO-induced fibrosis in mice. A, Time course of UUO induced fibrosis in WT and GSTA4 KO mice. PAS staining was performed in WT and *GSTA4* KO mice after UUO at different time points. The contralateral kidney was used as a control. The density of red color in PAS staining is proportional to the area of fibrosis. B. The statistical analysis of the cells with intracellular vacuolization after UUO in WT and GSTA4 KO mice. C. Fibronectin was upregulated in *GSTA4* KO mice after 3 day-long UUO. D. Western blot analysis of collagen I expression in WT and *GSTA4* KO mice after UUO for 3 and 7 days. *GAPDH* was used for the loading control. E. The positive areas of collagen I staining in WT and *GSTA4* KO mice.

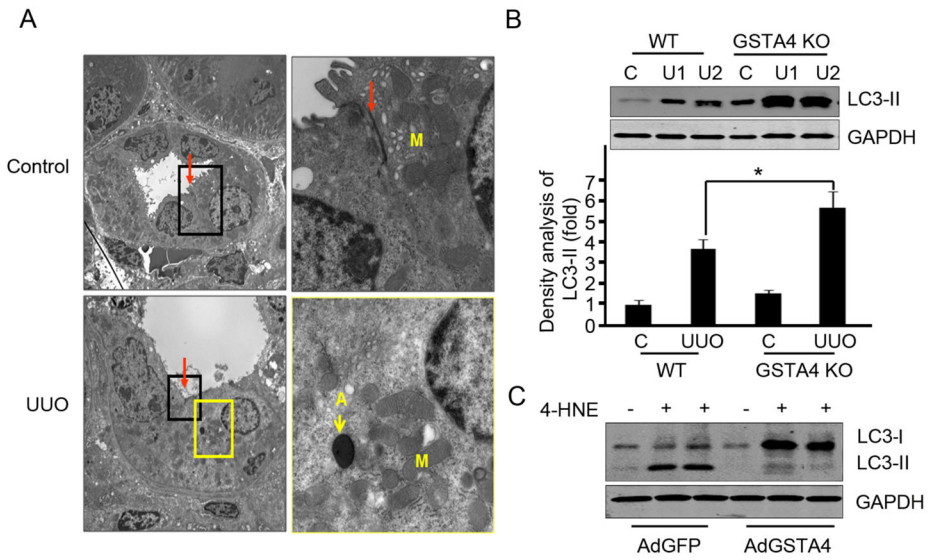

Figure 4.

GSTA4 overexpression protects against 4-HNE-induced autophagy activation. A. Transmission electron microscopy images were taken after 7 days UUO. The inset rectangular frames in the left panels delineate the areas that are amplified in the right panels. Arrows show the tight junction (red) and autophagy (yellow). A, autophagy; M, mitochondria. B. LC3-II was detected by Western blot analysis. The proteins were prepared from kidneys after UUO performed in WT and *GSTA4* KO mice. The bar graph represents the density of LC3-II band after normalizing to the loading control. C. LC3-II was analyzed in tubular cells with or without GSTA4 adenovirus infection. Media containing 4-HNE (25 μM) was incubated with cells for 24 h before the cell lysates were prepared for Western blot analysis.

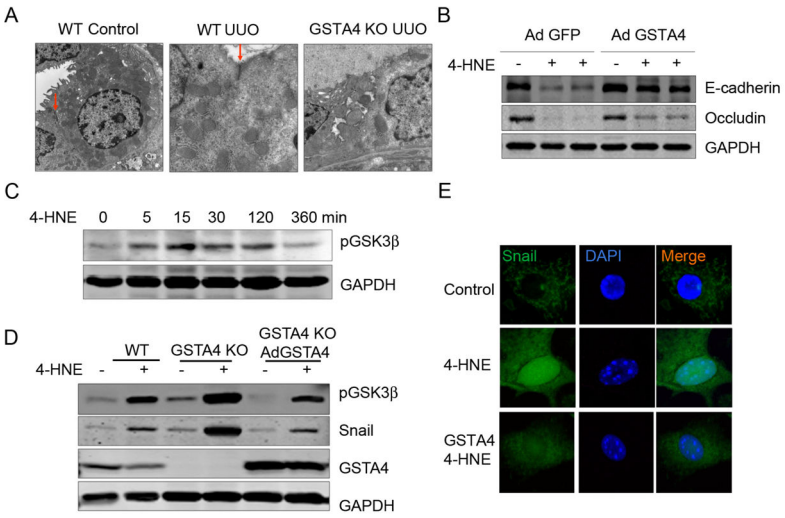

Figure 5.

GSTA4 protects against 4-HNE-induced tubular cell junction molecule loss in vitro. A, Transmission electron microscopy images were taken of samples harvested 7 days after UUO. The arrows show the tight junction (red). B. The statistic analysis of panel A, the number of cell junction complex in 4 areas of the images was counted. C. GSTA4 prevents 4-HNE–mediated decrease in the junction molecules Occludin and E-cadherin in the tubular cells. Tubular cells with or without GSTA4 overexpression were treated with 4-HNE for 24 h and the levels of Occludin and E-cadherin were detected by Western blot. The densitometric data was shown in the lower panel. D and E. The time-dependent effect of 4-HNE include increased GSK3β phosphorylation (C) and Snail expression (D) that can be blocked by *GSTA4* overexpression. F. *GSTA4* overexpression blocked 4-HNE-induced nuclear translocation of Snail. Tubular cells were transfected with Flag-Snail with or without the GSTA4 expression plasmids. The cells was treated with 4-HNE for 6 h and immunostaining were performed to detect the Flag-Snail protein.

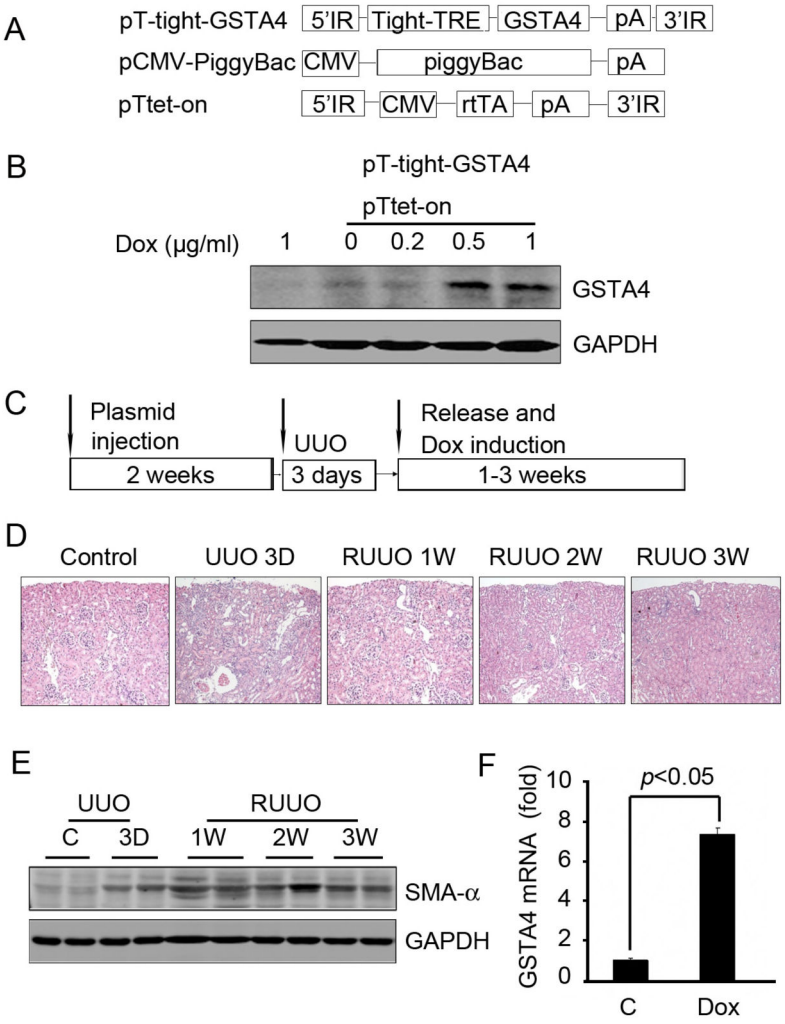

Figure 6.

Inducible *GSTA4* gene expression in the R-UUO model. A. Plasmids used in the injection were pT-tight-GSTA4 (*GSTA4* gene regulated by tetracycline repressor element); pCMV-*piggyBac* (the *piggyBac* transposase driven by the CMV promoter), and pTtet-on (the CMV promoter-driven regulatory protein that will induce expression from the tight promoter only when bound to doxycycline). B. Inducible GSTA4 expression in tubular cells. The cells were transfected with the plasmids pT-tight-GSTA4 and pTtet-on. Different doses of doxycycline (0–1 μg/ml) were added to the cells for 24 h. Western blot analysis of protein extracts of cells given GSTA4 plasmids was performed. C. Schematic of the delivery of the transposons used to create inducible GSTA4 in kidneys. Plasmids containing 20 μg each of the pT-tight-GSTA4, pCMV-*piggyBac*, and pTtet-on plasmids in Mirus QR solution were mixed and injected into renal vein. The GSTA4 and Tet-on genes were integrated into the mouse kidney genomic DNA by the transposase. UUO was performed after 2 weeks. The clamp was released after 3 day UUO and doxycycline was administered immediately after the clamp release. Kidneys were collected at the indicated time points for analysis. D. Morphology changes were determined by H & E staining. E. Western blot analysis of the SMA-α level in collected kidneys. F. Real time RT-PCR detection of inducible GSTA4

expression after doxycycline treatment for 3 weeks in kidneys that were injected with transposase and vector or GSTA4 inducible plasmids.

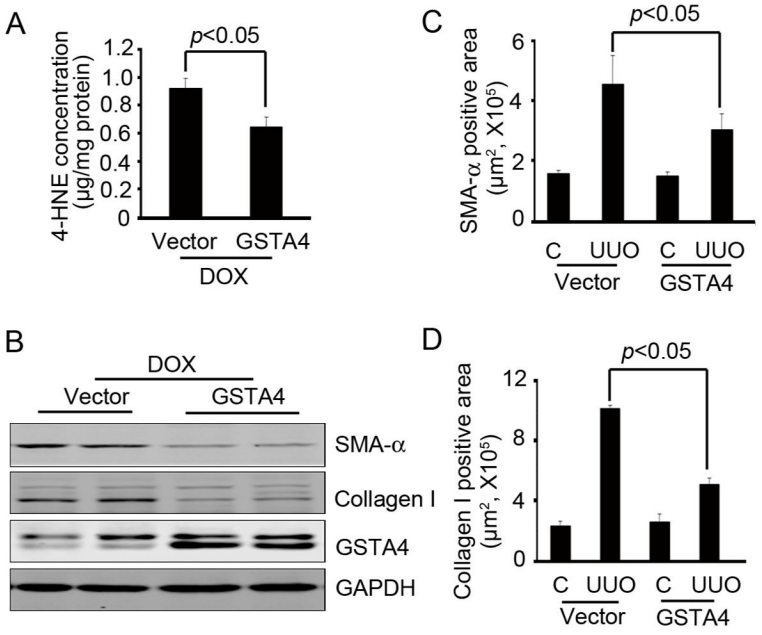

Figure 7.

Inducible expression of GSTA4 accelerates recovery of UUO-induced fibrosis. The kidneys were collected after the treatment indicated in Fig. 6C, A. 4-HNE level was decreased in R-UUO samples after GSTA4 induction. B. Western blot analysis of the effect of GSTA4 on the expression of SMA-α and collagen I in kidney with UUO. C. SMA-α positive area in R-UUO were decreased in GSTA4 induction. D. The collagen I deposition was measured and was less in the GSTA4 induction group.

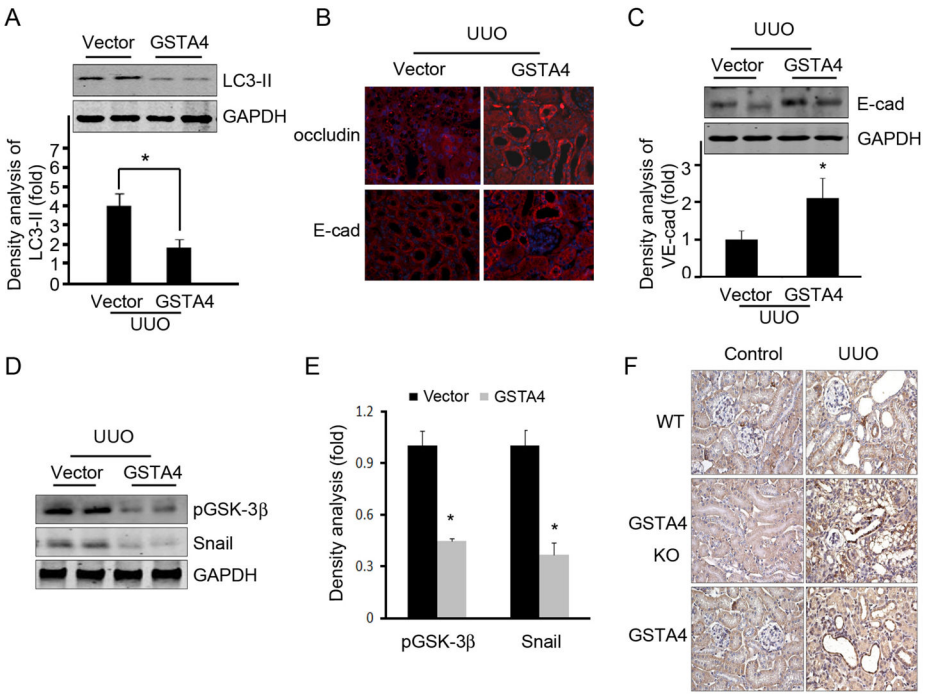

Figure 8.

Overexpression of GSTA4 prevents UUO-mediated autophagy and tubular cell damage. A. GSTA4 overexpression in kidney suppresses UUO-induced autophagy activation. LC3-II was detected by Western blot analysis. The proteins were prepared from kidneys after UUO was performed in vector control and in GSTA4 overexpressing mice. The bar graph represents the density of LC3-II after normalization to the loading control. B and C. Overexpression of GSTA4 attenuated UUO-induced junction marker loss in tubular cells. The levels of expression of E-cadherin and Occludin were analyzed by immunofluorescent staining (B) and Western blot. D to F. Overexpression of GSTA4 prevents GSK3β phosphorylation and Snail expression in the kidneys. The phosphorylated GSK3β and expression of Snail in the kidneys was analyzed by Western blot (D) and immunostaining (F) after UUO for 3 days in WT, *GSTA4* KO, and in GSTA4 overexpressing mice. Densitometric analysis was performed based on the Western blot results (E).